

Advanced Channel Decomposition Techniques in OTFS: A GSVD Approach for Multi-User Downlink

Omid Abbassi Aghda^{1,2}, Oussama Ben Haj Belkacem^{1,3}, Dou Hu⁴, João Guerreiro^{1,2}, Nuno Souto^{1,5},
Michal Szczachor^{2,6}, and Rui Dinis^{1,2}

¹Instituto de Telecomunicações, Lisboa, Portugal

²Universidade Nova de Lisboa, Monte da Caparica, 2829-516 Caparica, Portugal

³Innov'Com Laboratory, Sup'Com, University of Carthage, Tunis 1054, Tunisia

⁴University of Tokyo, Tokyo, Japan

⁵ ISCTE-Instituto Universitário de Lisboa, 1649-026 Lisbon, Portugal

⁶Nokia, Wroclaw, Poland

Abstract—In this paper, we propose a multi-user downlink system for two users based on the orthogonal time frequency space (OTFS) modulation scheme. The design leverages the generalized singular value decomposition (GSVD) of the channels between the base station and the two users, applying precoding and detection matrices based on the right and left singular vectors, respectively. We derive the analytical expressions for three scenarios and present the corresponding simulation results. These results demonstrate that, in terms of bit error rate (BER), the proposed system outperforms the conventional multi-user OTFS system in two scenarios when using minimum mean square error (MMSE) equalizers or precoder, both for perfect channel state information and for a scenario with channel estimation errors. In the third scenario, the design is equivalent to zero-forcing (ZF) precoding at the transmitter.

Index Terms—OTFS, GSVD, MIMO, Multi-User, System Design, Performance Evaluation

I. INTRODUCTION

Reliable communication in the sixth generation (6G) of wireless networks is crucial for high-speed users. Orthogonal time frequency space (OTFS) modulation is specifically designed for this scenario, as it multiplexes information in the delay-Doppler (DD) domain, enabling it to track both the delay and the Doppler spread of the channel [1], [2]. However, several challenges must be addressed when dealing with multiple access (MA) in OTFS.

Orthogonal multiple access (OMA) methods in OTFS modulation have been explored in various studies. The authors in [3] proposed multiplexing in the DD domain and allocating different DD bins to different users. This method is simple on the transmitter side; however, each user must cancel out interference from other users at the receiver. To address this, guard intervals can be considered between the multiplexed data

in the DD domain, which results in lower spectral efficiency. In [4], time-frequency (TF) resource allocation is considered for OTFS modulation, where information symbols are multiplexed and interleaved in the DD domain so that their corresponding TF domain is contiguous. In the study [5], an uplink MA scenario was proposed based on Orthogonal Frequency Division Multiplexing (OFDM) modulation for single input single output (SISO) systems. They demonstrated that the concatenated signal from all symbols at the base station (BS) is equivalent to a single-user OTFS system. Their work was further extended in a subsequent study [6], where they investigated the uplink scenario for multiple input multiple output (MIMO)

Similarly, non-orthogonal multiple access (NOMA) has been explored in the context of OTFS modulation. The authors in [7] proposed a deep learning-based signal detection method for a two-user downlink SISO-NOMA system. In [8], a robust beamforming method is proposed for a downlink MIMO system with two users. This method multiplexes the low mobility user's information in the TF domain while ensuring the high mobility user meets the minimum requirements by multiplexing its information in the DD domain. In [9], the authors utilize an interference alignment (IA) matrix as a precoder to reduce inter-user interference (IUI) in a multi user (MU) MIMO-OTFS downlink system. They also consider singular value decomposition (SVD) and precoding to diagonalize the channel matrix and perform data detection.

The other remaining challenge in OTFS modulation is the equalization, despite much research on the subject. The input-output equation of the transceiver in the DD domain is modeled as a 2 dimensional (2D) phase-rotated convolution between the transmitted signal and the channel impulse response in the DD domain [2]. Due to this 2D convolution, and compared to OFDM, which allows for a low-complexity single-tap equalizer, OTFS channel equalization and data detection remains challenging due to high computational complexity. In high-speed scenarios, frequency domain equalization (FDE) is ineffective for OTFS. Unlike in low-mobility scenarios with

This work was conducted within the MiFuture project, which has received funding from the European Union's Horizon Europe (HE) Marie Skłodowska-Curie Actions Doctoral Networks (MiFuture HORIZON-MSCA-2022-DN-01 and YAHYA/6G HORIZON-MSCA-2022-PF-01) under Grant Agreement number 101119643. It was partially supported by Fundação para a Ciência e Tecnologia and Instituto de Telecomunicações under the project UIDB/50008/2020 DOI:10.54499/UIDB/50008/2020.

single carrier modulation (SCM), where a single-tap equalizer can be used for FDE, this approach does not work for OTFS. It is worth mentioning that the performance of the OTFS system is not affected by user speed, unlike high mobility system designs in OFDM and SCM, if an adequate equalization or detection technique is applied.

The generalized singular value decomposition (GSVD) decomposition was initially proposed in [10], with a more comprehensive definition provided in [11]. Additionally, the authors in [12] introduced the Higher Order GSVD (HO-GSVD) to decompose more than two matrices. In [13], the author utilized GSVD to separate a wireless channel for two users into the private channel (PC) and common channel (CC), offering a complete overview of both definitions of the GSVD decomposition.

Our contribution in this paper is the development of a precoding and detection scheme for a MU MIMO-OTFS system based on GSVD decomposition. This decomposition allows us to reduce the channel matrix to a diagonal form, thereby avoiding the need to handle a 2D circular convolution at the receiver. We then evaluate the performance of the proposed system and compare it with other MU MIMO systems, including block diagonalization (BD) precoding, minimum mean square error (MMSE) precoding, and MMSE equalization. Our proposed method demonstrates superiority over these mentioned methods.

Notation: In the rest of this paper Boldface upper case, Boldface lower case, and normal lower case indicate matrices, vectors, and scalars, respectively. Notations $(\cdot)^H$, $(\cdot)^T$, and $\text{vec}(\cdot)$ are used to represent the Hermitian, transpose, and column-wise vectorization. The notation $\mathbf{A}_{\{:,1:k\}}$ indicates the selection of 1^{st} to the k^{th} column of the matrix \mathbf{A} . \mathbf{I}_k , $\mathbf{0}_k$, and $\mathbf{0}_{k \times r}$ denote the identity matrix of size $k \times k$, the zero matrix of size $k \times k$, and the zero matrix of size $k \times r$, respectively.

II. OTFS SYSTEM MODEL

In OTFS modulation, the DD domain is discretized into an $M \times N$ grid, where M and N are the number of bins along the delay and Doppler axes, respectively. In this grid, the l^{th} bin ($l = 0, 1, \dots, M-1$) corresponds to a delay of $\tau = \frac{l}{B}$, and the k^{th} bin ($k = 0, 1, \dots, N-1$) corresponds to a Doppler shift of $\nu = \frac{k}{T_f}$. Here, B and T_f represent the bandwidth and the frame duration, respectively. Accordingly, the sub-carrier spacing for the corresponding TF domain and the OTFS sub-symbol duration are $\Delta f = \frac{B}{M}$ and $T_s = \frac{T_f}{N}$, respectively, such that $T_s \Delta f = 1$.

A. SISO System model

In SISO-OTFS, information precoded symbols are multiplexed in the DD grid, represented by the matrix $\mathbf{X} \in \mathbb{C}^{M \times N}$. This signal passes through the equivalent DD channel representation, and the received signal in the DD domain is given by [14, Chapter 4]

$$\mathbf{y} = \mathbf{H}\mathbf{x} + \mathbf{n}, \quad (1)$$

where $\mathbf{x} = \text{vec}\{\mathbf{X}^T\} \in \mathbb{C}^{MN \times 1}$ and $\mathbf{y} = \text{vec}\{\mathbf{Y}^T\} \in \mathbb{C}^{MN \times 1}$, with $\mathbf{Y} \in \mathbb{C}^{M \times N}$ being the DD representation of the received

signal. The channel matrix $\mathbf{H} \in \mathbb{C}^{MN \times MN}$ represents the equivalent DD channel between \mathbf{x} and \mathbf{y} .

B. MIMO MA System Model

The same DD domain discretization used for SISO is applied to the MIMO case. We consider a downlink system with C antennas at the base station and 2 users, each equipped with G antennas. For simplicity, we focus on 2 users in this paper.¹ The signal representation in the DD domain for the c^{th} antenna is $\mathbf{X}_c \in \mathbb{C}^{M \times N}$ for $c = 1, 2, \dots, C$.

The received signal at the g^{th} antenna for 1^{st} and 2^{nd} user is given by

$$\begin{cases} \mathbf{y}_{g,1} = \mathbf{H}_{g,1,1}\mathbf{x}_1 + \mathbf{H}_{g,1,2}\mathbf{x}_2 + \dots + \mathbf{H}_{g,1,C}\mathbf{x}_C + \mathbf{n}_{g,1} \\ \mathbf{y}_{g,2} = \mathbf{H}_{g,2,1}\mathbf{x}_1 + \mathbf{H}_{g,2,2}\mathbf{x}_2 + \dots + \mathbf{H}_{g,2,C}\mathbf{x}_C + \mathbf{n}_{g,2}, \end{cases} \quad (2)$$

where $\mathbf{y}_{g,1}, \mathbf{y}_{g,2} \in \mathbb{C}^{MN \times 1}$ for $g = 1, 2, \dots, G$. In (2), $\mathbf{H}_{g,1,c} \in \mathbb{C}^{MN \times MN}$ and $\mathbf{H}_{g,2,c} \in \mathbb{C}^{MN \times MN}$ are the DD channel matrices between the c^{th} antenna of the transmitter and the g^{th} antenna of the receiver for the 1^{st} and 2^{nd} user, respectively. For this paper, we assume a rich physical environment characterized by a high number of multipath components. This ensures that the matrices $\mathbf{H}_{g,1,c}$ and $\mathbf{H}_{g,2,c}$ are full-rank, i.e., $\text{rank}(\mathbf{H}_{g,1,c}) = \text{rank}(\mathbf{H}_{g,2,c}) = MN$. The vector \mathbf{x}_c for $c = 1, 2, \dots, C$ is the transmitted signal vector, such that $\mathbf{x}_c = \text{vec}(\mathbf{X}_c^T) \in \mathbb{C}^{MN \times 1}$.

The received signals from all antennas for each user can be concatenated, allowing (2) to be rewritten as

$$\begin{cases} \mathbf{y}_1 = \mathbf{H}_1\mathbf{x} + \mathbf{n}_1 \\ \mathbf{y}_2 = \mathbf{H}_2\mathbf{x} + \mathbf{n}_2. \end{cases} \quad (3)$$

The received vector for the 1^{st} user, \mathbf{y}_1 , and the transmitted vector from the BS, \mathbf{x} , are given by

$$\mathbf{y}_1 = \begin{bmatrix} \mathbf{y}_{1,1} \\ \mathbf{y}_{2,1} \\ \vdots \\ \mathbf{y}_{G,1} \end{bmatrix} \in \mathbb{C}^{MNG \times 1}, \mathbf{x} = \begin{bmatrix} \mathbf{x}_1 \\ \mathbf{x}_2 \\ \vdots \\ \mathbf{x}_C \end{bmatrix} \in \mathbb{C}^{MNC \times 1}. \quad (4)$$

The channel matrix between the BS and the 1^{th} user is modeled as

$$\mathbf{H}_1 = \begin{bmatrix} \mathbf{H}_{1,1,1} & \mathbf{H}_{1,1,2} & \dots & \mathbf{H}_{1,1,C} \\ \mathbf{H}_{2,1,1} & \mathbf{H}_{2,1,2} & \dots & \mathbf{H}_{2,1,C} \\ \vdots & \ddots & \ddots & \vdots \\ \mathbf{H}_{G,1,1} & \mathbf{H}_{G,1,2} & \dots & \mathbf{H}_{G,1,C} \end{bmatrix} \in \mathbb{C}^{MNG \times MNC}. \quad (5)$$

Similarly, \mathbf{y}_2 and \mathbf{H}_2 represent the received vector and channel matrix for the 2^{nd} user.

III. GSVD DECOMPOSITION, PRECODING AND DETECTION MATRIX

The precoding matrix $\mathbf{P} \in \mathbb{C}^{MNC \times MNC}$ is defined such that $\mathbf{x} = \frac{1}{\rho}\mathbf{P}\mathbf{s}$. In this context, $s = \text{rank}\{\mathbf{H}\}/(MN)$, where

¹While this work can be extended to multiple users with different numbers of antennas using HO-GSVD [12] [13].

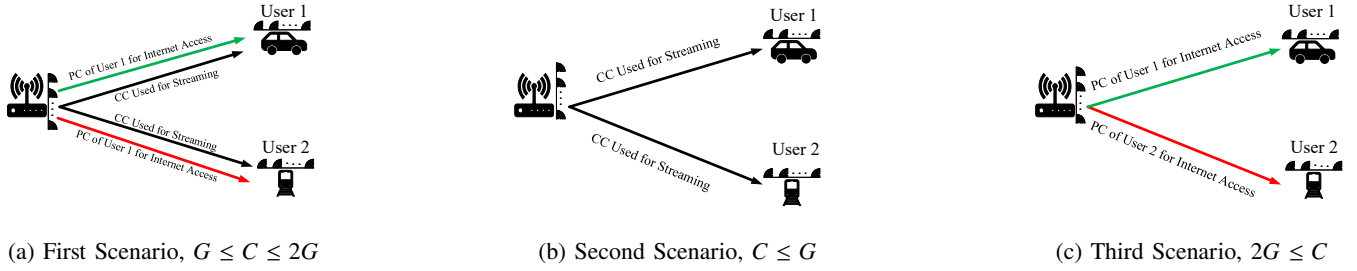


Fig. 1: Schematic of different scenarios in GSVD-based channel decomposition for precoding and detection matrix design.

$\mathbf{H} = [\mathbf{H}_1^T, \mathbf{H}_2^T]^T$, representing the number of data streams. The scalar ρ is a normalization factor used to ensure constant average power at the transmitter². Vector $\mathbf{s} \in \mathbb{C}^{MNs \times 1}$ denotes the information quadrature amplitude modulation (QAM) symbols. In the receiver, we use the vectors $\mathbf{r}_1 = \rho \mathbf{D}_1 \mathbf{y}_1$ and $\mathbf{r}_2 = \rho \mathbf{D}_2 \mathbf{y}_2$, with $\mathbf{r}_1, \mathbf{r}_2 \in \mathbb{C}^{MNG \times 1}$, as the signal for detection purposes. The detection matrices for the first and second users are $\mathbf{D}_1, \mathbf{D}_2 \in \mathbb{C}^{MNG \times MNG}$, respectively. We define the precoding and detection matrices in the following of this section.

Based on the GSVD, the channel matrices \mathbf{H}_1 and \mathbf{H}_2 are decomposed as

$$\begin{cases} \mathbf{H}_1 = \mathbf{U}_1 \mathbf{\Sigma}_1 \mathbf{V}^H \\ \mathbf{H}_2 = \mathbf{U}_2 \mathbf{\Sigma}_2 \mathbf{V}^H. \end{cases} \quad (6)$$

Here, $\mathbf{U}_1, \mathbf{U}_2 \in \mathbb{C}^{MNG \times MNG}$ are unitary matrices, $\mathbf{\Sigma}_1, \mathbf{\Sigma}_2 \in \mathbb{C}^{MNG \times MNs}$ are block diagonal matrices, and $\mathbf{V} \in \mathbb{C}^{MNC \times MNs}$ is the joint matrix (JM).

We consider three scenarios: $G \leq C \leq 2G$, $C \leq G$, and $2G \leq C$. The detection matrices for each scenario are $\mathbf{D}_1 = \mathbf{U}_1^H$ and $\mathbf{D}_2 = \mathbf{U}_2^H$. Moreover, the structures of $\mathbf{\Sigma}_1$, $\mathbf{\Sigma}_2$, and \mathbf{V} , and consequently the precoding matrix \mathbf{P} , are explained in each scenario.

A. Scenario I: $G \leq C \leq 2G$

In this case, we have $s = C$ data streams, and \mathbf{V} is a square invertible matrix. Therefore, we choose the precoding matrix as $\mathbf{P} = (\mathbf{V}^H)^{-1}$. By substituting \mathbf{P} , \mathbf{D}_1 , \mathbf{D}_2 , and the GSVD decomposition of (6) into (3), we obtain

$$\begin{cases} \mathbf{r}_1 = \mathbf{U}_1^H \mathbf{y}_1 = \mathbf{U}_1^H \mathbf{U}_1 \mathbf{\Sigma}_1 \mathbf{V}^H (\mathbf{V}^H)^{-1} \mathbf{s} + \mathbf{U}_1^H \mathbf{n}_1 \\ \mathbf{r}_1 = \mathbf{U}_2^H \mathbf{y}_2 = \mathbf{U}_2^H \mathbf{U}_2 \mathbf{\Sigma}_2 \mathbf{V}^H (\mathbf{V}^H)^{-1} \mathbf{s} + \mathbf{U}_2^H \mathbf{n}_2. \end{cases} \quad (7)$$

Here,

$$\mathbf{\Sigma}_1 = \begin{bmatrix} \mathbf{I}_r & \mathbf{0}_{r \times t} & \mathbf{0}_r \\ \mathbf{0}_{t \times r} & \mathbf{C}_1 & \mathbf{0}_{t \times r} \end{bmatrix}, \mathbf{\Sigma}_2 = \begin{bmatrix} \mathbf{0}_{t \times r} & \mathbf{C}_2 & \mathbf{0}_{t \times r} \\ \mathbf{0}_r & \mathbf{0}_{r \times t} & \mathbf{I}_r \end{bmatrix}, \quad (8)$$

where $r = MN(C - G)$, $t = MN(2G - C)$, and $\mathbf{C}_1, \mathbf{C}_2 \in \mathbb{C}^{t \times t}$ are diagonal matrices with the CC coupling coefficients for user 1 and user 2, respectively. Matrix \mathbf{I}_r represents the PC for the first and second users. Since the detection matrices \mathbf{D}_1 and \mathbf{D}_2 are unitary, there is no noise enhancement in the

receiver due to the terms $\mathbf{U}_1^H \mathbf{n}_1$ and $\mathbf{U}_2^H \mathbf{n}_2$. Moreover, equation (7) can be simplified to

$$\begin{cases} \mathbf{r}_1 = \mathbf{\Sigma}_1 \mathbf{s} + \mathbf{n}'_1 \\ \mathbf{r}_2 = \mathbf{\Sigma}_2 \mathbf{s} + \mathbf{n}'_2, \end{cases} \quad (9)$$

where $\mathbf{n}'_1 = \mathbf{U}_1^H \mathbf{n}_1$ and $\mathbf{n}'_2 = \mathbf{U}_2^H \mathbf{n}_2$. Since in (9) the matrices $\mathbf{\Sigma}_1$ and $\mathbf{\Sigma}_2$ are diagonal, the information symbols \mathbf{s} can be easily detected with a single tap MMSE equalizer.

Observing carefully (9) and comparing it with (8), it can be seen that users 1 and 2 receive r private data streams through their own PC. In fact, they do not have access to the other user's information. At the same time, both users can access t common data streams through CC channel. In figure 1a, it can be observed an applicable scenario where users 1 and 2 are using a broadcasting service simultaneously. They utilize CC for shared information while each user also receives their private and personal information through PC.

B. Scenario II: $C \leq G$

Similar to scenario I, there are $s = C$ data streams, and \mathbf{V} is a square matrix. The precoding matrix is defined as in scenario I. The input-output relation for the processed received signal is given by (9). Matrices $\mathbf{\Sigma}_1$ and $\mathbf{\Sigma}_2$ are as follows

$$\mathbf{\Sigma}_1 = \begin{bmatrix} \mathbf{C}_1 \\ \mathbf{0}_{r \times MNC} \end{bmatrix}, \mathbf{\Sigma}_2 = \begin{bmatrix} \mathbf{C}_2 \\ \mathbf{0}_{r \times MNC} \end{bmatrix}, \quad (10)$$

where $\mathbf{C}_1, \mathbf{C}_2 \in \mathbb{C}^{MNC \times MNC}$ are diagonal matrices with the CC coefficients for user 1 and user 2. In this scenario we have $r = G - C$. By comparing (10) and (9) it can be noted the first C antennas in each receiver can be used to extract the information. Moreover, although the last r antennas in each receiver appear unused for data detection, they contribute to diversity gain. This gain is integrated into the precoding matrix \mathbf{P} , improving its performance in interference cancellation. A broadcasting scenario where each user wants to have access to the same information, as illustrated in figure 1b.

C. Scenario III: $2G \leq C$

In this case, the number of data streams is $s = 2G$, allowing us to allocate $s/2$ streams for each user. The matrix \mathbf{V} is not square and can be decomposed as follows

$$\mathbf{V}^H = [\mathbf{W}^H \mathbf{R}, \mathbf{0}_{MN \times t}] \mathbf{Q}^H. \quad (11)$$

²The calculation of the normalization factor ρ is fully explained in [13].

Here, $\mathbf{W} \in \mathbb{C}^{MNs \times MNs}$ and $\mathbf{Q} \in \mathbb{C}^{MNC \times MNC}$ are unitary matrices, $t = C - 2G$, and $\mathbf{R} \in \mathbb{C}^{MNs \times MNs}$ is an invertible matrix with the singular values of the matrix \mathbf{H} . The precoding matrix is defined as³ $\mathbf{P} = \mathbf{Q}_{\{:,1:MNs\}} \mathbf{R}^{-1} \mathbf{W} \in \mathbb{C}^{MNC \times MNs}$. At the receiver, after applying the detection matrix for each user, we have

$$\begin{cases} \mathbf{r}_1 = \mathbf{U}_1^H \mathbf{U}_1 \underbrace{\Sigma_1}_{\mathbf{V}^H} [\mathbf{W}^H \mathbf{R}, \mathbf{0}_{MNs \times t}] \underbrace{\mathbf{Q}^H \mathbf{Q}_{\{:,1:MNs\}}}_{\mathbf{P}} \mathbf{R}^{-1} \mathbf{W} \mathbf{s} + \mathbf{n}'_1 \\ \mathbf{r}_2 = \mathbf{U}_2^H \mathbf{U}_2 \Sigma_2 [\mathbf{W}^H \mathbf{R}, \mathbf{0}_{MNs \times t}] \mathbf{Q}^H \mathbf{Q}_{\{:,1:MNs\}} \mathbf{R}^{-1} \mathbf{W} \mathbf{s} + \mathbf{n}'_2. \end{cases} \quad (12)$$

The multiplication of matrix \mathbf{V}^H by precoding matrix \mathbf{P} is the identity matrix \mathbf{I}_s , so (12) will reduce to (9), with

$$\Sigma_1 = [\mathbf{I}_{MNG} \quad \mathbf{0}_{MNG}], \Sigma_2 = [\mathbf{0}_{MNG} \quad \mathbf{I}_{MNG}]. \quad (13)$$

Comparing (13) and (9), it can be noted that each user can detect the information symbols solely through the PC, with no common information transmitted via the CC. Consequently, none of the users have access to each other's information, as illustrated in figure 1c.

IV. SIMULATION RESULTS

In this section, we evaluate the performance of the proposed GSVD decomposition. The simulation parameters are listed in Table I. The maximum speed of the environment is set to $v_{\max} = 500$ km/h. Consequently, the relative maximum Doppler shift and the normalized Doppler shift are calculated as $\nu_{\max} = \frac{v_{\max} \times f_c}{\text{light speed}} = 1853$ Hz and $k_{\max} = \nu_{\max} T_f = 0.9883$, respectively. The information bits are mapped into information symbols using 4-QAM modulation. For each scenario, we compared our method with various MU-MIMO schemes. In scenario I, we used the BD precoding scheme proposed in [15] followed by MMSE equalizer at the receiver. In scenario II, we employed an MMSE equalizer at the receiver. Lastly, in scenario III, we considered MMSE precoding.

Fig. 2 represents the bit error rate (BER) curve versus signal to noise ratio (SNR). The results are shown for Scenario I, where $G \leq C \leq 2G$, with $C = 4$ and $G = 3$. As mentioned in Section III, this scenario includes both PC and CC for the GSVD-based OTFS system. The simulation results indicate a significant gap between PC and CC, with PC demonstrating superior performance. In the GSVD system, there is 1 PC and 2 CCs, whereas in the BD-MMSE approach, there are 2 PCs. Comparing our method with BD precoding and MMSE equalizer, we observe better performance with the BD-MMSE approach, but it only transmits two data streams, limiting common information transmission.

Fig. 3 illustrates Scenario II, where $C \leq G$ and $C = 3$, $G = 4$. In this scenario, only CC is present. The BER performance of the GSVD-based OTFS system for each user is inferior to MMSE equalization. This is attributed to the fact that some CC coefficients are quite small. However, when analyzing each data stream individually rather than collectively, it is observed that the BER for two of the streams surpasses that of MMSE

TABLE I: Simulation parameters

Parameters	Values
Carrier frequency	$f_c = 4$ GHz
Sub-carrier spacing	$\Delta_f = 15$ kHz
(M, N)	(16, 8)
Tap delays (ns)	[0, 30, 150, 310, 370, 710, 1090, 1730, 2510]
Tap powers (dB)	-[0, 1.5, 1.4, 3.6, 0.6, 9.1, 7, 12, 16.9]
Max. speed	500 km/h

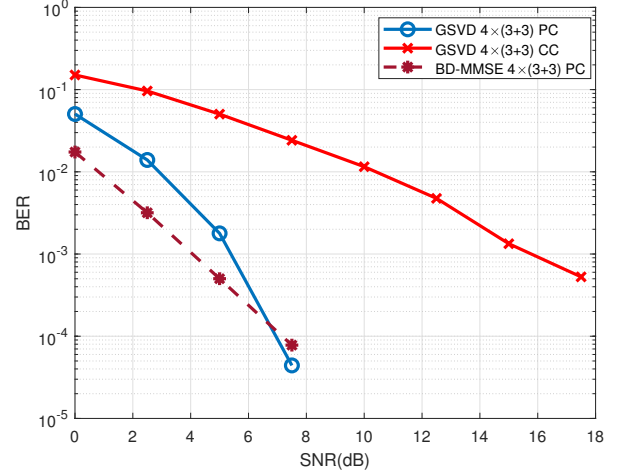


Fig. 2: BER vs SNR for Scenario I, comparing GSVD-based precoding and MMSE precoding.

equalization, while one stream performs worse than MMSE. This suggests that the proposed scheme can perform effectively with the application of an appropriate coding scheme such as low-density parity check (LDPC). Furthermore, the GSVD-based method offers the advantage of channel equalization at the receiver using a single-tap equalizer, thereby transforming the channel matrix into a diagonal form. This simplifies the process significantly, as handling large non-diagonal matrices in OTFS modulation has always been challenging.

Fig. 4 illustrates Scenario III, where $2G \leq C$ and $C = 5$, $G = 2$. In this scenario, our proposed method outperforms the MMSE precoding technique. It is evident that in this scenario, we only have PC. As with other scenarios, the performance of User 1 and User 2 for both MMSE-based precoding and GSVD-based precoding remains the same.

In Fig. 5, we show the system's performance with channel estimation errors. With $C = 2$ and $G = 2$, this case fits either Scenario I or II. If the time domain channel coefficient is h_k , we model the estimated channel coefficient using $h_{k,\text{est}} = \rho h_k + \epsilon$, where $0 \leq \rho \leq 1$ and $E\{\epsilon^2\} = (1 - \rho^2)E\{|h_k|^2\}$ (with $E\{\cdot\}$ indicating the expected value). The figure shows the superiority of the proposed method compared to MMSE equalization in the presence of channel estimation errors for the stream with better channel conditions, and performance almost similar to the MMSE method for the stream with worse conditions.

³For simulations, this simplifies to $\mathbf{P} = \mathbf{V}(\mathbf{V}^H \mathbf{V})^{-1}$, as GSVD beamforming simplifies to zero forcing (ZF) transmission when the $2G \leq C$ [13].

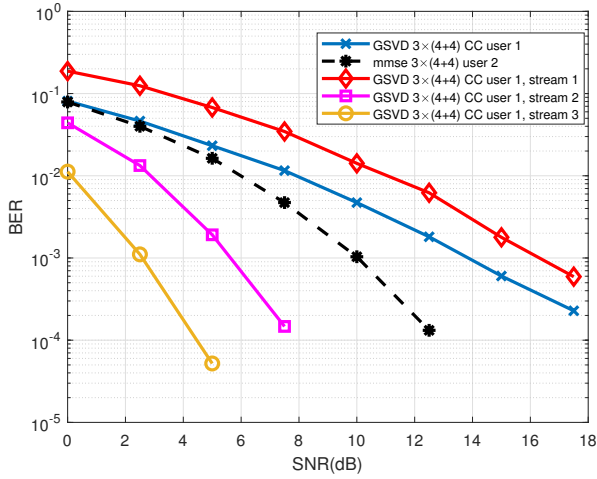


Fig. 3: BER vs SNR for Scenario II, comparing GSVD-based precoding and MMSE equalization.

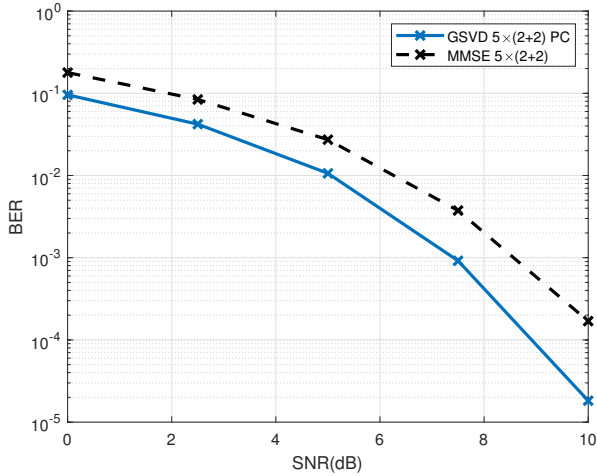


Fig. 4: BER vs SNR for Scenario III, comparing GSVD-based precoding and MMSE precoding.

V. CONCLUSION AND RESEARCH OPPORTUNITIES

In this paper, we proposed the adoption of the GSVD decomposition for a downlink two-user MIMO-OTFS system and derived analytical expressions for three scenarios. The system is based on GSVD decomposition of each user's channel and on applying a precoding and detection matrix. The simulation results indicate the superiority of the proposed GSVD scheme compared to conventional MMSE. The extension of the GSVD for two-user into HO-GSVD for more users in uplink and downlink scenarios can be an interesting future work path.

REFERENCES

[1] R. Hadani, S. Rakib, M. Tsatsanis, A. Monk, A. J. Goldsmith, A. F. Molisch, and R. Calderbank, "Orthogonal time frequency space modulation," in *2017 IEEE Wireless Communications and Networking Conference (WCNC)*, 2017, pp. 1–6.

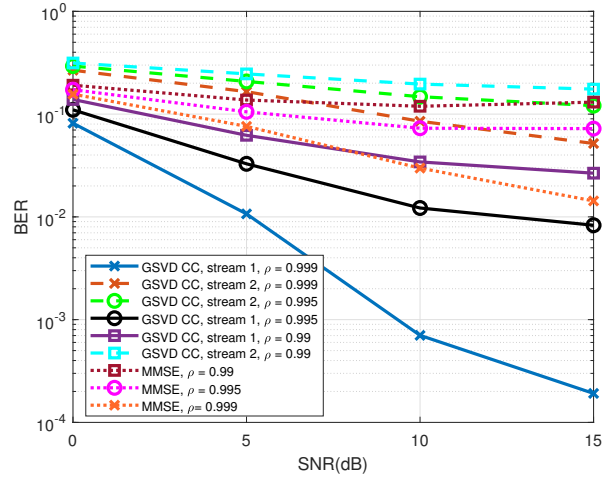


Fig. 5: BER vs SNR for Scenario II, comparing GSVD-based precoding and MMSE equalization in the presence of estimation error.

[2] P. Raviteja, K. T. Phan, Y. Hong, and E. Viterbo, "Interference cancellation and iterative detection for orthogonal time frequency space modulation," *IEEE Transactions on Wireless Communications*, vol. 17, no. 10, pp. 6501–6515, 2018.

[3] S. Rakib and R. Hadani, "Multiple access in wireless telecommunication system for high-mobility applications," Patent US9 722 741B1, August, 2017, uS Patent.

[4] V. Khammammetti and S. K. Mohammed, "Otf-based multiple-access in high doppler and delay spread wireless channels," *IEEE Wireless Communications Letters*, vol. 8, no. 2, pp. 528–531, 2019.

[5] B. V. S. Reddy, C. Velampalli, and S. S. Das, "Performance analysis of multi-user ofds, ofsm, and single carrier in uplink," *IEEE Transactions on Communications*, vol. 72, no. 3, pp. 1428–1443, 2024.

[6] B. V. Sudhakar Reddy, S. S. Das, C. Velampalli, and G. S. Sanyal, "Multi-user ofds with multi-antenna transmission," in *2024 15th International Conference on Computing Communication and Networking Technologies (ICCCNT)*, 2024, pp. 1–7.

[7] I. Umakoglu, M. Namdar, and A. Basgumus, "Deep learning-assisted signal detection for ofds-noma systems," *IEEE Access*, vol. 12, pp. 119 105–119 115, 2024.

[8] Z. Ding, "Robust beamforming design for ofds-noma," *IEEE Open Journal of the Communications Society*, vol. 1, pp. 33–40, 2020.

[9] S. Yang, H. Liu, Y. Zhou, Z. Ma, and P. Fan, "Joint precoding based on interference alignment and svd for mu-mimo ofds with mrc detector," *IEEE Wireless Communications Letters*, vol. 13, no. 10, pp. 2717–2721, 2024.

[10] C. F. Van Loan, "Generalizing the singular value decomposition," *SIAM Journal on Numerical Analysis*, vol. 13, no. 1, pp. 76–83, 1976.

[11] C. C. Paige and M. A. Saunders, "Towards a generalized singular value decomposition," *SIAM Journal on Numerical Analysis*, vol. 18, no. 3, pp. 398–405, Jun. 1981.

[12] I. Kempf, P. J. Goulart, and S. R. Duncan, "A higher-order generalized singular value decomposition for rank-deficient matrices," *SIAM Journal on Matrix Analysis and Applications*, vol. 44, no. 3, pp. 1047–1072, 2023. [Online]. Available: <https://doi.org/10.1137/21M1443881>

[13] D. Senaratne and C. Tellambura, "Gsvd beamforming for two-user mimo downlink channel," *IEEE Transactions on Vehicular Technology*, vol. 62, no. 6, pp. 2596–2606, 2013.

[14] Y. Hong, T. Thaj, and E. Viterbo, *Delay-Doppler Communications: Principles and Applications*. Academic Press, 2022.

[15] B. Bandemer, M. Haardt, and S. Visuri, "Linear mmse multi-user mimo downlink precoding for users with multiple antennas," in *2006 IEEE 17th International Symposium on Personal, Indoor and Mobile Radio Communications*, 2006, pp. 1–5.